

# Widespread Anthropogenic Nitrogen in Northwestern Pacific Ocean Sediment

Haryun Kim,<sup>†</sup> Kitack Lee,<sup>\*,†,‡</sup> Dhong-Il Lim,<sup>‡</sup> Seung-Il Nam,<sup>§</sup> Tae-Wook Kim,<sup>||</sup> Jin-Yu T. Yang,<sup>†</sup> Young Ho Ko,<sup>†</sup> Kyung-Hoon Shin,<sup>⊥</sup> and Eunil Lee<sup>#</sup>

<sup>†</sup>Division of Environmental Science and Engineering, Pohang University of Science and Technology, Pohang 37673, Korea

<sup>‡</sup>South Sea Research Institute, Korea Institute of Ocean Science and Technology, Jangmok 53201, Korea

<sup>§</sup>Arctic Research Center, Korea Polar Research Institute, Incheon 21990, Korea

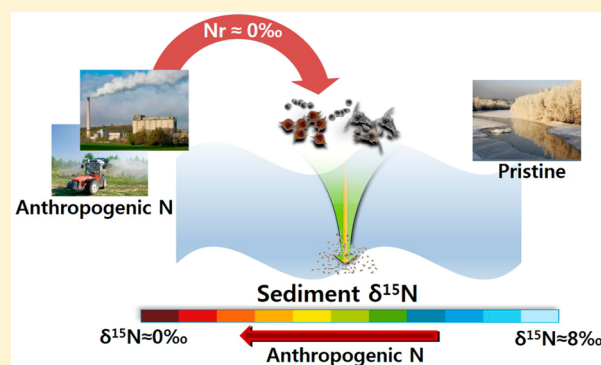
<sup>||</sup>Department of Marine Science, Incheon National University, Incheon 22012, Korea

<sup>⊥</sup>Department of Marine Sciences and Convergent Technology, Hanyang University, Ansan 15588, Korea

<sup>#</sup>Ocean Research Division, Korea Hydrographic and Oceanographic Agency, Busan 49111, Korea

## Supporting Information

**ABSTRACT:** Sediment samples from the East China and Yellow seas collected adjacent to continental China were found to have lower  $\delta^{15}\text{N}$  values (expressed as  $\delta^{15}\text{N} = [^{15}\text{N}:^{14}\text{N}_{\text{sample}}/^{15}\text{N}:^{14}\text{N}_{\text{air}} - 1] \times 1000\text{‰}$ ; the sediment  $^{15}\text{N}:^{14}\text{N}$  ratio relative to the air nitrogen  $^{15}\text{N}:^{14}\text{N}$  ratio). In contrast, the Arctic sediments from the Chukchi Sea, the sampling region furthest from China, showed higher  $\delta^{15}\text{N}$  values (2–3‰ higher than those representing the East China and the Yellow sea sediments). Across the sites sampled, the levels of sediment  $\delta^{15}\text{N}$  increased with increasing distance from China, which is broadly consistent with the decreasing influence of anthropogenic nitrogen ( $\text{N}^{\text{ANTH}}$ ) resulting from fossil fuel combustion and fertilizer use. We concluded that, of several processes, the input of  $\text{N}^{\text{ANTH}}$  appears to be emerging as a new driver of change in the sediment  $\delta^{15}\text{N}$  value in marginal seas adjacent to China. The present results indicate that the effect of  $\text{N}^{\text{ANTH}}$  has extended beyond the ocean water column into the deep sedimentary environment, presumably via biological assimilation of  $\text{N}^{\text{ANTH}}$  followed by deposition. Further, the findings indicate that  $\text{N}^{\text{ANTH}}$  is taking over from the conventional paradigm of nitrate flux from nitrate-rich deep water as the primary driver of biological export production in this region of the Pacific Ocean.



## INTRODUCTION

The increasing use of nitrogen (N) fertilizers and fossil fuels has more than doubled the oceanic loads of reactive N (i.e.,  $\text{NO}_y$  +  $\text{NH}_x$  and dissolved organic forms) since the industrial revolution.<sup>1</sup> In particular, the marginal seas of the densely populated northeast Asian countries have been found to be vulnerable to the impact of anthropogenic nitrogen ( $\text{N}^{\text{ANTH}}$ ),<sup>(2)</sup> which mainly emanates from fossil fuel combustion and N fertilizers, and its influence has been found to extend far into the open North Pacific Ocean.<sup>3</sup> However, to our knowledge, no observational evidence has been reported showing a link between changes in  $\text{N}^{\text{ANTH}}$  input to the marine environment and corresponding changes in sediment N biogeochemistry by planktonic assimilation of  $\text{N}^{\text{ANTH}}$  and subsequent deposition in the sediments.

The sediment  $^{15}\text{N}:^{14}\text{N}$  ratio relative to the air nitrogen  $^{15}\text{N}:^{14}\text{N}$  ratio ( $\delta^{15}\text{N}$ ) is a potentially useful measure of human N influence. The usefulness of this isotope ratio stems from intrinsic N isotope signatures of various N sources. For

example, the N produced by vehicles ( $\delta^{15}\text{N}$  −4 to −1‰),<sup>4</sup> fossil fuel burning ( $\delta^{15}\text{N}$  ~ 0‰),<sup>5</sup> and inorganic fertilizers ( $\delta^{15}\text{N}$  −2 to 2‰)<sup>5</sup> is more depleted in the heavier  $^{15}\text{N}$  isotope compared with the  $^{15}\text{N}$  of the nitrate in the present-day deep ocean ( $\delta^{15}\text{N}$ -nitrate ~ 5‰).<sup>6</sup>

Therefore, the addition of  $\text{N}^{\text{ANTH}}$  to the marine environment lowers the  $\delta^{15}\text{N}$  in both the water column and phytoplankton and thereby lowering the sediment  $\delta^{15}\text{N}$ . Previous measurements of the N isotope composition of organic matter in sediments from several lakes under the influence of  $\text{N}^{\text{ANTH}}$  showed decrease in  $\delta^{15}\text{N}$  during the past 150 years.<sup>7</sup> This trend of decreasing  $\delta^{15}\text{N}$  approximately corresponds to the increase in production of industrial N during the same period. However, the majority of previous studies investigating the influence of  $\text{N}^{\text{ANTH}}$  were primarily focused on riverine and estuarine

Received: October 20, 2016

Revised: April 11, 2017

Accepted: May 2, 2017

Published: May 2, 2017

**Table 1.** Surface Sediment Ages for the East China Sea, the Yellow Sea, the East Sea, the Pacific Coast of Japan, the Okhotsk Sea, the Bering Sea, and the Arctic Ocean

basin	location	age (yr) ( $\pm$ SD)	no. of samples	method	ref
East China Sea	31° N–35.5° N 123° E–126.5° E	8 $\pm$ 10	9	$^{210}\text{Pb}_{\text{ex}}$	18, 19
Yellow Sea	35° N–36° N 123.2° E–124.8° E	8 $\pm$ 2	2	$^{210}\text{Pb}_{\text{ex}}$	19
East Sea	35.5° N–37° N 129.5° E–131.5° E	17 $\pm$ 10	9	$^{210}\text{Pb}_{\text{ex}}$	52, 53
Pacific coast of Japan	44.5° N, 145° E	13 $\pm$ 7 <sup>a</sup>	3	AMS $^{14}\text{C}$	54, 55
Okhotsk Sea	49.5° N–51° N 146° E–152° E	42 $\pm$ 15 <sup>a</sup>	3	AMS $^{14}\text{C}$	56
Bering Sea	52° N–57° N 162° E–177° W	20	1	$^{326}\text{Ra}$	57
Arctic Ocean Shelf	70° N–75° N 165° W–175° W	8 $\pm$ 4	2	$^{210}\text{Pb}_{\text{ex}}$	58
Arctic Ocean Basin	>75° N	>1000		$^{210}\text{Pb}_{\text{ex}}$	58

<sup>a</sup>Age values were calculated by multiplying 1 cm layer of sediment by reciprocals of the sedimentation rates ( $\text{cm kyr}^{-1}$ ) based on the  $^{14}\text{C}$  method. Note that no age determination was performed on shelf sediments from the Pacific coast of Japan and Okhotsk Sea where our samples were collected. Use of the  $^{14}\text{C}$  method may lead to errors in ages estimated for shelf surface sediments. However, the estimated ages are likely to be upper limits because the sedimentation rates in the shelf regions, where all of our samples were collected, are probably considerably higher than those in the offshore regions where the sedimentation rate was determined using the  $^{14}\text{C}$  method.

environments.<sup>8–10</sup> Moreover, the studies performed on the marginal sea sedimentary environments were aimed to identify key internal processes (e.g., denitrification or surface nitrate availability to phytoplankton) influencing the sediment  $\delta^{15}\text{N}$ .<sup>11–13</sup> We are unaware of any study investigating the influence of  $\text{N}^{\text{ANTH}}$  on more remote marginal sea and open ocean sedimentary environments, where riverine  $\text{N}^{\text{ANTH}}$  inputs are insignificant but atmospheric  $\text{N}^{\text{ANTH}}$  inputs can be considerable. Previous studies probably overlooked the possibility of an influence of  $\text{N}^{\text{ANTH}}$  on such remote marine sedimentary environments, because such an influence was thought to be negligible.<sup>11–13</sup>

In this study, we evaluated the influence of  $\text{N}^{\text{ANTH}}$  on the ocean sedimentary environment through analyses of the N isotope composition of bulk organic matter. Analyses were undertaken at various locations in the study area with rates of  $\text{N}^{\text{ANTH}}$  input from atmospheric deposition and river ranging from high to near-zero. Geographically, the locations correspond to the East China and Yellow seas (highest  $\text{N}^{\text{ANTH}} \sim 258 \text{ mmol m}^{-2} \text{ yr}^{-1}$ ),<sup>2,14,15</sup> the East Sea (Sea of Japan;  $\text{N}^{\text{ANTH}} \sim 52 \text{ mmol m}^{-2} \text{ yr}^{-1}$ ),<sup>16</sup> the Pacific coast of Japan ( $\text{N}^{\text{ANTH}} \sim 20 \text{ mmol m}^{-2} \text{ yr}^{-1}$ ),<sup>16</sup> the Okhotsk Sea ( $\text{N}^{\text{ANTH}} \sim 5 \text{ mmol m}^{-2} \text{ yr}^{-1}$ ),<sup>16</sup> the Bering Sea ( $\text{N}^{\text{ANTH}} \sim 3 \text{ mmol m}^{-2} \text{ yr}^{-1}$ ),<sup>16</sup> and the Arctic Ocean (lowest  $\text{N}^{\text{ANTH}} \sim 1 \text{ mmol m}^{-2} \text{ yr}^{-1}$ ).<sup>16</sup>

## MATERIALS AND METHODS

**Sediment Sampling Methods.** We collected one surface sediment sample from each of 227 sites for the East China ( $n = 88$ ) and Yellow ( $n = 139$ ) seas using a grab sampler or a box corer over various Korea Oceanographic Institute expeditions conducted since 2000 (Tables S1 and S2). Loss of the core-top of the sample due to use of a grab sampler was likely minimal due to the fine-grained cohesive aggregate compositions that are prevalent in these basins.<sup>17</sup> Moreover, even if the core-top material was disturbed, the high sedimentation rates in these basins would mean that the sediments below the core-top would likely still contain substantial amounts of  $\text{N}^{\text{ANTH}}$ .<sup>18,19</sup> Only 16 sediment samples for the East Sea ( $n = 8$ ) and the

Arctic Ocean ( $n = 8$ ) were taken using a multicorer between 2010 and 2013 (Tables S1 and S2). All sediment samples were stored in an onboard freezer and prior to analysis samples were freeze-dried for 4 days and then ground to powder with a mortar and pestle.

In our analysis we also used additional 231  $\delta^{15}\text{N}$  data from 231 distinct sites in the East China Sea ( $n = 71$ ), the Pacific coast of Japan ( $n = 102$ ), the Okhotsk Sea ( $n = 22$ ), the Bering Sea ( $n = 30$ ), and the Arctic Ocean ( $n = 6$ ) obtained from the Nitrogen Cycle in the Ocean, Past and Present database (NICOPP; <https://www.ncdc.noaa.gov/paleo/pubs/nicopp/nicopp.html>).<sup>20</sup> Only key information about sampling methods and sites is summarized in Table S1, and more detailed information can be found in the work of Tesdal et al.<sup>20</sup>

**N and C Isotope Analysis for Sediments.** For N isotope analysis, approximately 70 mg of sediment sample was weighed and wrapped in a tin capsule. N isotope composition ( $\delta^{15}\text{N}$ ) was measured using a PDZ Europa ANCA-GSL elemental analyzer interfaced to a PDZ Europa 20-20 isotope ratio mass spectrometer (Sercon Ltd., Cheshire, UK) at the Stable Isotopes Facility Center of the University of California at Davis.<sup>21</sup> N isotope values were expressed in  $\delta$  (‰) with respect to the atmospheric nitrogen standard, which was calibrated against National Institute of Standards and Technology Standard reference materials (IAEA-N1, IAEA-N2, IAEA-N3, USGS-40, and USGS-41). The measurement error was reported to be less than 0.3‰.<sup>22</sup> The sampling locations of our sediment samples and the corresponding  $\delta^{15}\text{N}$  values are listed in Table S2. For the NICOPP  $\delta^{15}\text{N}$  data used in our analysis, the analytical methods used and the corresponding sampling locations are summarized in Table S1 and can also be found in the work of Tesdal et al.<sup>20</sup>

The carbon isotope ratio ( $\delta^{13}\text{C}$ ) was also measured for selected sediment samples for sites located more than 50 km from the mouth of a major river ( $n = 7$  for the East China Sea,  $n = 5$  for the Yellow Sea,  $n = 4$  for the East Sea, and  $n = 4$  for the Arctic Ocean). For  $\delta^{13}\text{C}$  analysis, sediment samples were treated with 1 M HCl for 3 days in a precombusted (500 °C) glass beaker to remove  $\text{CaCO}_3$ , then washed with distilled

water several times, and dried at 60 °C for 3 days. Approximately 70 mg of dried sample was weighed and wrapped in a silver capsule. The  $\delta^{13}\text{C}$  was measured using a Vision EA Stable Isotope Ratio Mass Spectrometer System with Elemental Analyzer (Isoprime, Manchester, UK)<sup>21</sup> at the National Instrumentation Center for Environmental Management at Seoul National University. The results were expressed in  $\delta$  (‰) with respect to the Pee Dee Belemnite standard, which was calibrated against National Institute of Standards and Technology Standard reference materials (USGS-40 and USGS-41). The measurement error was reported to be less than 0.2‰.<sup>22</sup>

**Total Nitrogen (TN) and Total Organic Carbon (TOC) Analysis for Sediments.** The concentrations of TN, total carbon (TC), and total inorganic carbon (TIC) in the dried and ground sediment samples were measured using a Thermo Electron Corp. Flash EA 1112 Series NC Soil Analyzer for TN and TC and a  $\text{CO}_2$  coulometer (model CM5014, UIC Inc.) for TIC (Waltham, MA, USA).<sup>23</sup> TOC concentrations were calculated by subtracting TIC from TC.

**Atmospheric Nitrogen Deposition and Surface Ocean Nitrate Data.** The atmospheric nitrogen deposition data ( $n = 457$ ) were obtained from the Oak Ridge National Laboratory Distributed Active Archive Center (<https://daac.ornl.gov/>),<sup>16</sup> and the surface ocean nitrate concentration data ( $n = 472$ ) were obtained from the World Ocean Atlas 2013 (<http://www.nodc.noaa.gov/OCS/woa13/woa13data.html>).<sup>24</sup>

## RESULTS AND DISCUSSION

**Surface Sediment  $\delta^{15}\text{N}$  (‰) in the Marginal Seas of the Northwestern Pacific Ocean.** A key requirement in studies on the effect of  $\text{N}^{\text{ANTH}}$  on sediment  $\delta^{15}\text{N}$  is that the ages of surface sediments (<1 cm depth) sampled across the study area are similar. The published rates of sedimentation for all basins in the study area indicated that, except for some open Arctic basin samples, most surface sediments compared in this study are young and similar in age ( $17 \pm 12$  years), indicating that most sediment samples used in this study contained fresh organic matter that had recently accumulated (Table 1).

The  $\delta^{15}\text{N}$  value (‰) for surface sediment samples was lowest for the East China Sea ( $5.0 \pm 0.8\text{‰}$ ) and progressively increased in a northeast direction from the East Sea ( $5.4 \pm 0.3\text{‰}$ ) to the Bering Sea ( $6.9 \pm 1.5\text{‰}$ ) and the Arctic Ocean ( $8.0 \pm 0.7\text{‰}$ ); these locations are increasingly distant from the major  $\text{N}^{\text{ANTH}}$  source continent (China) (Figures 1 and 2). The northeastward increase in surface sediment  $\delta^{15}\text{N}$  is inversely related to the northeastward decrease in the deposition of  $\text{N}^{\text{ANTH}}$  (Figure 3). A similar inverse correlation was also evident between the deposition of  $\text{N}^{\text{ANTH}}$  and the  $\delta^{15}\text{N}$  trend of sinking particulate organic matter (sinking POM) collected in the overlying water column close to the sediments ( $\delta^{15}\text{N} = 2.9\text{--}4.2\text{‰}$  for the East China Sea sinking POM and  $9.4\text{--}13.9\text{‰}$  for the Bering Sea sinking POM) (inset in Figure 3). Although sinking POM  $\delta^{15}\text{N}$  values are not exactly equivalent to surface sediment  $\delta^{15}\text{N}$  values collected from the Bering Sea, the inverse relationship between sinking POM  $\delta^{15}\text{N}$  and  $\text{N}^{\text{ANTH}}$  input obtained across our study area provides further evidence supporting the dilution effect of  $\text{N}^{\text{ANTH}}$  on the water column  $\delta^{15}\text{N}$ , which leads to reductions in sinking POM  $\delta^{15}\text{N}$  and eventually sediment  $\delta^{15}\text{N}$ . Other studies also showed that sediment or POM  $\delta^{15}\text{N}$  values from more pristine regions (near Hawaii or South Atlantic Ocean) had 8.1 to 11.5‰ (Table S3),<sup>25–27</sup> whereas  $\delta^{15}\text{N}$ -nitrate or ammonium values for  $\text{N}^{\text{ANTH}}$

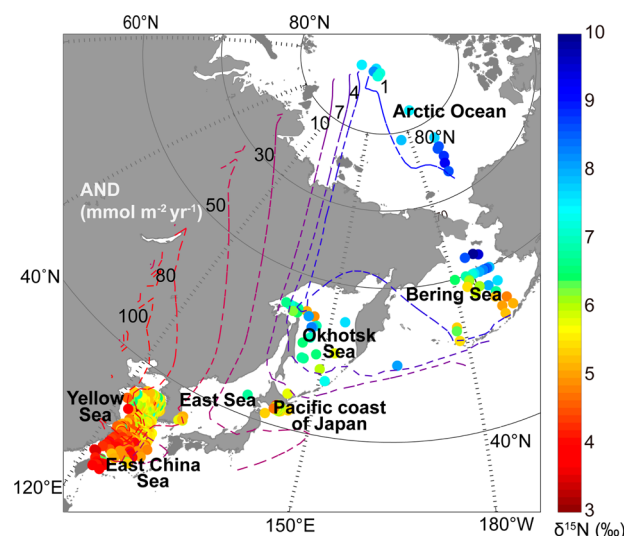


**Figure 1.** Sediment  $\delta^{15}\text{N}$  values in the study area. Surface sediment  $\delta^{15}\text{N}$  values (‰; colored circles) and atmospheric nitrogen deposition (AND;  $\text{mmol m}^{-2} \text{yr}^{-1}$ ; colored dashed lines) in the East China Sea, the Yellow Sea, the East Sea, the Pacific coast of Japan, the Okhotsk Sea, the Bering Sea, and the Arctic Ocean. The map was created using Matlab and Simulink (R2017a version).

deposition measured in the China<sup>28</sup> and the East Sea were  $<0\text{‰}$  (Table S4). Therefore, our observation of the increasing trend in sediment  $\delta^{15}\text{N}$  from the East China Sea to the Arctic Ocean can be associated with  $\text{N}^{\text{ANTH}}$  contamination.

**$\text{N}^{\text{ANTH}}$  Input Influencing Sediment  $\delta^{15}\text{N}$  (‰).** The marginal seas bordering the northwestern Pacific Ocean receive  $\text{N}^{\text{ANTH}}$  via atmospheric transport and deposition and from river and groundwater discharge.<sup>1,2</sup> Near-shore environments and marginal seas in close proximity to China receive large amounts of nitrate and ammonium ( $11 \times 10^{10} \text{ mol N yr}^{-1}$ ) from the Changjiang River,<sup>14</sup> whereas the Arctic Ocean only receives  $3.6 \times 10^9 \text{ mol N yr}^{-1}$  from the Mackenzie and Yukon rivers.<sup>29</sup> Thus, riverine nitrate probably contributes substantially to the  $\delta^{15}\text{N}$  signals in sedimentary environments in the vicinity of China, via assimilation by phytoplankton. However, it is difficult to distinguish the relative strengths of sources of  $\text{N}^{\text{ANTH}}$  because the effects of the major  $\text{N}^{\text{ANTH}}$  sources (fertilizers, fossil fuel burning, and organic wastes) vary considerably among location and over time.<sup>30</sup> Furthermore, riverine nitrate (as well as groundwater nitrate) is largely confined to coastal waters and thus does not leave a homogeneous footprint throughout the study area, making it difficult to establish correlations between  $\text{N}^{\text{ANTH}}$  input and sediment  $\delta^{15}\text{N}$  signal change. Therefore, we used atmospheric nitrogen deposition (AND) as a proxy for the total  $\text{N}^{\text{ANTH}}$  signal in the marine environment, because it probably best represents the basin-scale influence of  $\text{N}^{\text{ANTH}}$ .

To evaluate whether  $\text{N}^{\text{ANTH}}$  influences variations in sediment  $\delta^{15}\text{N}$  in the study area, the values for sediment  $\delta^{15}\text{N}$  were compared with the AND values in the surface ocean immediately above the sites where sediment  $\delta^{15}\text{N}$  values were determined. We found an inverse correlation between the sediment  $\delta^{15}\text{N}$  values and corresponding AND values throughout the study area (Figure 3). The high correlations between sediment  $\delta^{15}\text{N}$  and AND ( $r = 0.93$ ,  $p < 0.01$ ) are a strong indication that geographic variations in sediment  $\delta^{15}\text{N}$  values in the marginal seas of the northwest Pacific Ocean are probably caused by differences in  $\text{N}^{\text{ANTH}}$  input, resulting from

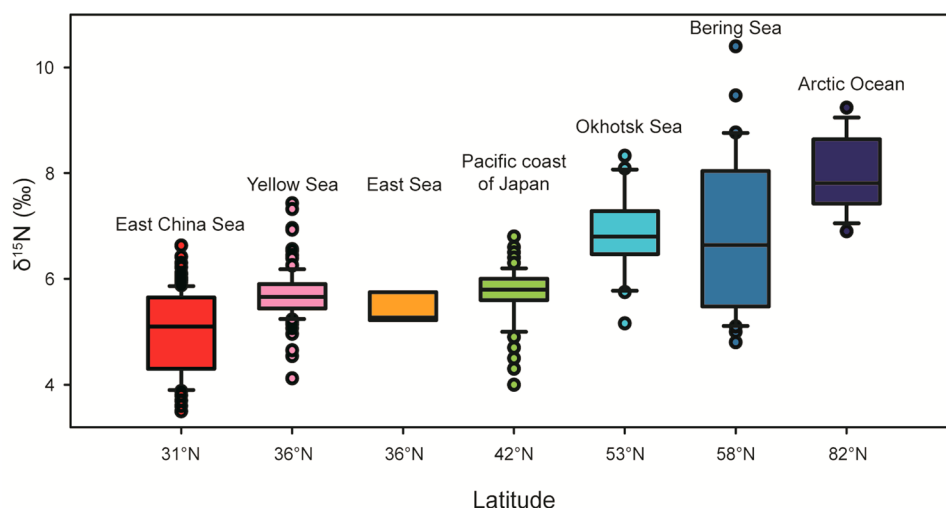


**Figure 2.** Mean sediment  $\delta^{15}\text{N}$  values (‰) for various basins.  $\delta^{15}\text{N}$  values (‰) for surface bulk sediments from the East China ( $n = 159$ ) and the Yellow ( $n = 139$ ) seas ( $\text{N}^{\text{ANTH}} \sim 258 \text{ mmol m}^{-2} \text{ yr}^{-1}$ ),<sup>2,14,15</sup> the East Sea ( $n = 8$ ;  $\text{N}^{\text{ANTH}} \sim 52 \text{ mmol m}^{-2} \text{ yr}^{-1}$ ),<sup>16</sup> the Pacific coast of Japan ( $n = 102$ ;  $\text{N}^{\text{ANTH}} \sim 20 \text{ mmol m}^{-2} \text{ yr}^{-1}$ ),<sup>16</sup> the Okhotsk Sea ( $n = 22$ ;  $\text{N}^{\text{ANTH}} \sim 5 \text{ mmol m}^{-2} \text{ yr}^{-1}$ ),<sup>16</sup> the Bering Sea ( $n = 30$ ;  $\text{N}^{\text{ANTH}} \sim 3 \text{ mmol m}^{-2} \text{ yr}^{-1}$ ),<sup>16</sup> and the Arctic Ocean ( $n = 14$ ;  $\text{N}^{\text{ANTH}} \sim 1 \text{ mmol m}^{-2} \text{ yr}^{-1}$ ).<sup>16</sup> Note that the  $\text{N}^{\text{ANTH}}$  input into the East China and Yellow Seas combined includes  $\text{N}^{\text{ANTH}}$  deposition and riverine inputs. The mid lines in the boxes indicate the median, and the lower and upper lines in the boxes are the first and third quartiles (respectively). The lower and upper whiskers indicate the minimum and maximum values (respectively), and the colored dots are outliers.

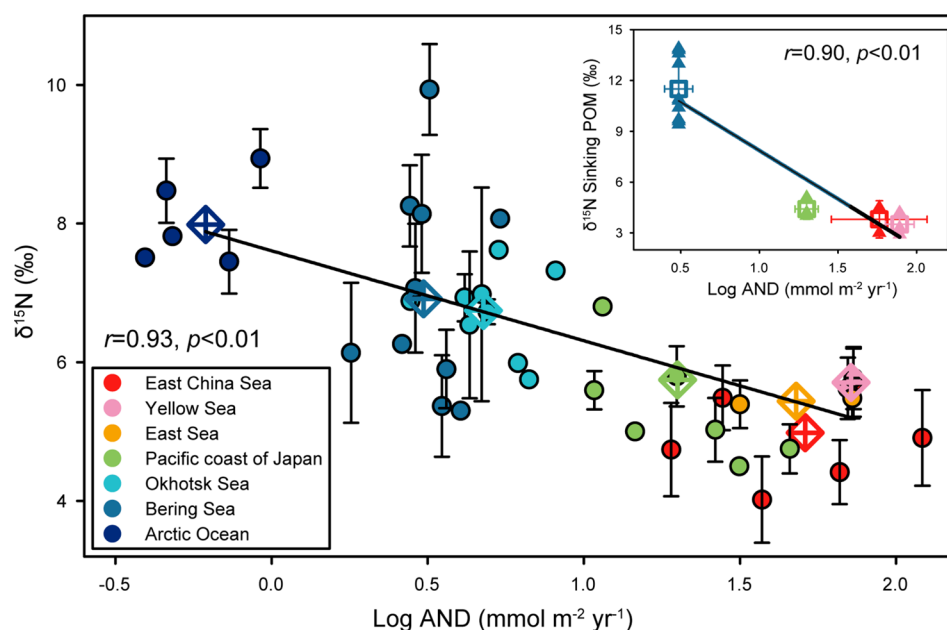


**Figure 3.** Plot of sediment  $\delta^{15}\text{N}$  values as a function of atmospheric nitrogen deposition (AND). AND data ( $\text{mmol m}^{-2} \text{ yr}^{-1}$ ) and sediment  $\delta^{15}\text{N}$  values (‰; colored circles) for the East China Sea, the Yellow Sea, the East Sea, the Pacific coast of Japan, the Okhotsk Sea, the Bering Sea, and the Arctic Ocean. Colored circles indicate the mean  $\delta^{15}\text{N}$  values ( $\pm\text{SD}$ ) for each pixel (latitude  $2.5^\circ \times$  longitude  $5^\circ$ ; the number of sediment samples ranges from 1 to 92), whereas open diamonds indicate individual basin means for  $\delta^{15}\text{N}$  and AND. The inset shows the AND and  $\delta^{15}\text{N}$  values (‰) for sinking particulate organic matter (Sinking POM) for the East China Sea ( $n = 2$ ),<sup>62</sup> the Yellow Sea ( $n = 3$ ),<sup>63</sup> the Pacific coast of Japan ( $n = 3$ ),<sup>34</sup> and the Bering Sea ( $n = 10$ )<sup>26</sup> sites. Colored triangles and open squares indicate individual sinking POM  $\delta^{15}\text{N}$  values and individual basin means for  $\delta^{15}\text{N}$  ( $\pm\text{SD}$ ), respectively.

the dramatic increase in  $\text{N}^{\text{ANTH}}$  emissions in northeast Asia since the 1970s.<sup>31,32</sup>

Another potentially powerful approach to assessing whether  $\text{N}^{\text{ANTH}}$  was responsible for the sediment  $\delta^{15}\text{N}$  values being lower in the East China and Yellow seas than the baseline value representing the pristine environment is to conduct a budget calculation of  $\text{N}^{\text{ANTH}}$  in the East China and Yellow seas combined, that is, to include the ocean regions under the greatest influence of  $\text{N}^{\text{ANTH}}$  in the study area. The accuracy of

this budget calculation depends on the validity of our assumption that any  $\delta^{15}\text{N}$ -nitrate change in the euphotic layer of the East China and Yellow seas, arising from the input of  $\text{N}^{\text{ANTH}}$ , will be comparably reflected in the sediment  $\delta^{15}\text{N}$  value via the complete utilization of all available nitrate (added  $\text{N}^{\text{ANTH}}$  and upwelled nitrate; another major source of nitrate for much of the ocean euphotic layer). Within the uncertainties of the measurements and estimations (Table 2), the  $\delta^{15}\text{N}$  decrease ( $\Delta\delta^{15}\text{N} \sim 1.9\text{‰}$ ) predicted for the water column from the



**Table 2. Impact of  $N^{ANTH}$  on the Seawater Dissolved Inorganic N (DIN) Isotope Values in the East China and Yellow Seas in the 2000s**

area (km <sup>2</sup> )	winter mixed layer depth (m) <sup>39</sup>	water column nitrate inventory <sup>a</sup> (T mol)	riverine DIN input <sup>b</sup> (T mol yr <sup>-1</sup> )	$N^{ANTH}$ deposition <sup>c</sup> (T mol yr <sup>-1</sup> )	predicted $\Delta\delta^{15}N^d$ (‰)	measured $\Delta\delta^{15}N^e$ (‰)
$6.6 \times 10^5$	30	0.07	0.13	0.04	1.9	$2.7 \pm 0.7$

<sup>a</sup>Calculated by integration of all nitrate contents to the average of bottom depths of the East China and Yellow seas. The annual mean of ocean nitrate for 1955 to 2012 yr were obtained from the World Ocean Atlas 2013 (<https://www.nodc.noaa.gov/OC5/woa13/woa13data.html>)<sup>24</sup> and represented all  $1^\circ$  latitude  $\times$   $1^\circ$  longitude pixels included in the basins specified. <sup>b</sup>The annual mean flux of DIN (nitrate and ammonium) from Chinese rivers (e.g., Changjiang, Liaohe, Haihe, Huang He rivers) and Korean rivers (e.g., Han, Keum, and Aproc rivers) for the 2000s.<sup>14,15</sup> <sup>c</sup>The mean  $N^{ANTH}$  deposition rate measured at the two sites (Cheju Island and Imsil) for the 2000s ( $0.065 \text{ mol m}^{-2} \text{ yr}^{-1}$ ) was extrapolated to the entire area of the East China and Yellow seas.<sup>2</sup> <sup>d</sup>Calculated using the following the mixing model equation<sup>60</sup>

$$F_\Sigma = \frac{m_x F_x + m_y F_y + m_z F_z}{(m_x + m_y + m_z)}$$

where  $F_\Sigma$  = the expected  $\delta^{15}N$  value (‰) after mixing  $F_x$ ,  $F_y$ , and  $F_z$ ,  $m_x$  = the total amount of water column nitrate inventory (T mol),  $F_x$  = the  $\delta^{15}N$ -nitrate isotopic ratio of the water column (We used the global mean of deep ocean values (5‰).<sup>6</sup>),  $m_y$  and  $m_z$  = total amounts of annual riverine DIN flux ( $m_y$ )<sup>14,15</sup> and annual air- $N^{ANTH}$  deposition ( $m_z$ ) (T mol),<sup>2</sup> and  $F_y$  and  $F_z$  = N isotopic values for riverine N ( $F_y = 3\%$ )<sup>61</sup> and  $N^{ANTH}$  deposition ( $F_z = 0\%$ ).<sup>4,5</sup> Predicted  $\Delta\delta^{15}N$  is the difference between  $F_x$  and  $F_\Sigma$ . <sup>e</sup>Measured differences in sediment  $\delta^{15}N$  between the baseline value and each basin ( $n = 298$  for the East China and Yellow seas and  $n = 8$  for the East Sea) and  $1\sigma$  from the mean of measured differences.

increase in  $N^{ANTH}$  content of the East China and Yellow seas was approximately consistent with the measured decrease ( $\Delta\delta^{15}N \sim 2.7\%$ ) in sediment  $\delta^{15}N$  of the same basins. The good correspondence between the predicted seawater  $\delta^{15}N$  decrease and measured sediment  $\delta^{15}N$  decrease constitutes compelling evidence that sediment  $\delta^{15}N$  in marginal seas with high loads of  $N^{ANTH}$  has already declined considerably, via the complete utilization of all available nitrate (added  $N^{ANTH}$  and upwelled nitrate) and subsequent deposition. The key assumption upon which our calculation is based (i.e., the complete utilization of nitrate in the study area) is more thoroughly confirmed in the next section.

#### Other Factors That May Influence Sediment $\delta^{15}N$ (‰).

The difference between the baseline  $\delta^{15}N$  values and those for sediments from individual basins may not be solely attributable to anthropogenic factors, because the production of organic matter at a location will alter the concentration of surface nitrate, which may in turn influence the planktonic  $\delta^{15}N$  value and hence the sediment  $\delta^{15}N$  value.<sup>13</sup> This effect is expected to be particularly important in phosphate-limited or Fe-limited and high nutrient and low chlorophyll environments (Gulf of Alaska, eastern Equatorial Pacific, and Southern oceans)<sup>12,13</sup> but not in nitrate-limited environments. Most of our study area, with the exception of a small region in the Bering Sea bordering the Fe-limited Gulf of Alaska, is known to be largely nitrate-limited,<sup>33</sup> and any added nitrate would be rapidly and completely utilized by phytoplankton during the spring bloom period; the low levels of nitrate ( $<2 \mu\text{M}$ ) in the study area in summer support this premise. For each basin we plotted sediment  $\delta^{15}N$  values as a function of the spring surface nitrate concentrations at locations where organic matter is produced. As the effect of  $N^{ANTH}$  input on sediment  $\delta^{15}N$  differed among the basins, we sought to minimize the effect of such basin-to-basin differences by normalizing each sediment  $\delta^{15}N$  value ( $\delta^{15}N_{\text{SAMP}}$ ) to the corresponding basin-mean  $\delta^{15}N$  value ( $\delta^{15}N_{\text{BASIN MEAN}}$ ). Regardless of the nitrate levels that phytoplankton encountered during spring blooms, we found no correlation between the surface nitrate concentrations and the normalized sediment  $\delta^{15}N$  values (Figure 4a). The absence of any correlation was a strong indication that the available nitrate was largely consumed during the spring bloom. Note that four samples taken near the boundary between the Gulf of Alaska

and the Bering Sea showed  $\delta^{15}N$  values  $\sim 1.9\%$  lower than the basin mean of  $6.9\%$ . This may be an indication of incomplete nitrate utilization due to intrusion of Fe-limited water from the Gulf of Alaska. However, these local effects did not affect the overall conclusion of our study.

The observed northeastward increase in sediment  $\delta^{15}N$  may be also derived from possible changes in  $\delta^{15}N$  as a result of site-specific microbial transformation of organic matter following deposition.<sup>34</sup> As microbial transformation of organic matter following deposition increases in the sedimentary environment, the ratio of TOC to TN is expected to increase along with the increasing  $\delta^{15}N$ . This is because microbial processes preferentially utilize protein over carbohydrate (i.e.,  $^{14}N$  over  $^{15}N$ ), making the residual organic matter more enriched in carbohydrate (increasing the TOC:TN ratio) and  $^{15}N$  (increasing the  $\delta^{15}N$ ).<sup>35</sup> In summary, the higher the TOC:TN ratio the greater is the postdepositional alteration. Therefore, we assessed the postdepositional change in  $\delta^{15}N$  by plotting the normalized sediment  $\delta^{15}N$  values as a function of the corresponding TOC:TN ratios in individual basins (Figure 4b). The normalized  $\delta^{15}N$  values did not change over a wide range of TOC:TN ratios among the various basins, indicating that microbial alteration of  $\delta^{15}N$  following deposition did not bias our  $\delta^{15}N$  values and thus did not affect interpretation of the results. Another approach to establishing whether sediment  $\delta^{15}N$  is affected by differences in microbial transformation of organic matter is by plotting the water depth at which sediment was sampled versus normalized sediment  $\delta^{15}N$ . The rationale behind this analysis is that organic matter in sediments at greater depth has spent longer in the water and hence will have undergone greater transformation.<sup>34</sup> However, we did not find any significant change in normalized  $\delta^{15}N$  as a function of water depth (Figure 4c). Therefore, we ruled out the possibility that the observed northeast increase in sediment  $\delta^{15}N$  values was due to microbial alteration of  $\delta^{15}N$  following deposition.

Marine  $N_2$  fixation cannot be completely ruled out as an alternative, albeit highly unlikely, explanation for the northeastward increase in sediment  $\delta^{15}N$ . This process generally produces organic matter depleted in  $^{15}N$  (i.e.,  $\delta^{15}N \sim 0\%$ ), which has the effect of reducing sediment  $\delta^{15}N$  values. Thus, the trend in sediment  $\delta^{15}N$  values could potentially be explained, at least in part, by a decrease in  $N_2$  fixation in the

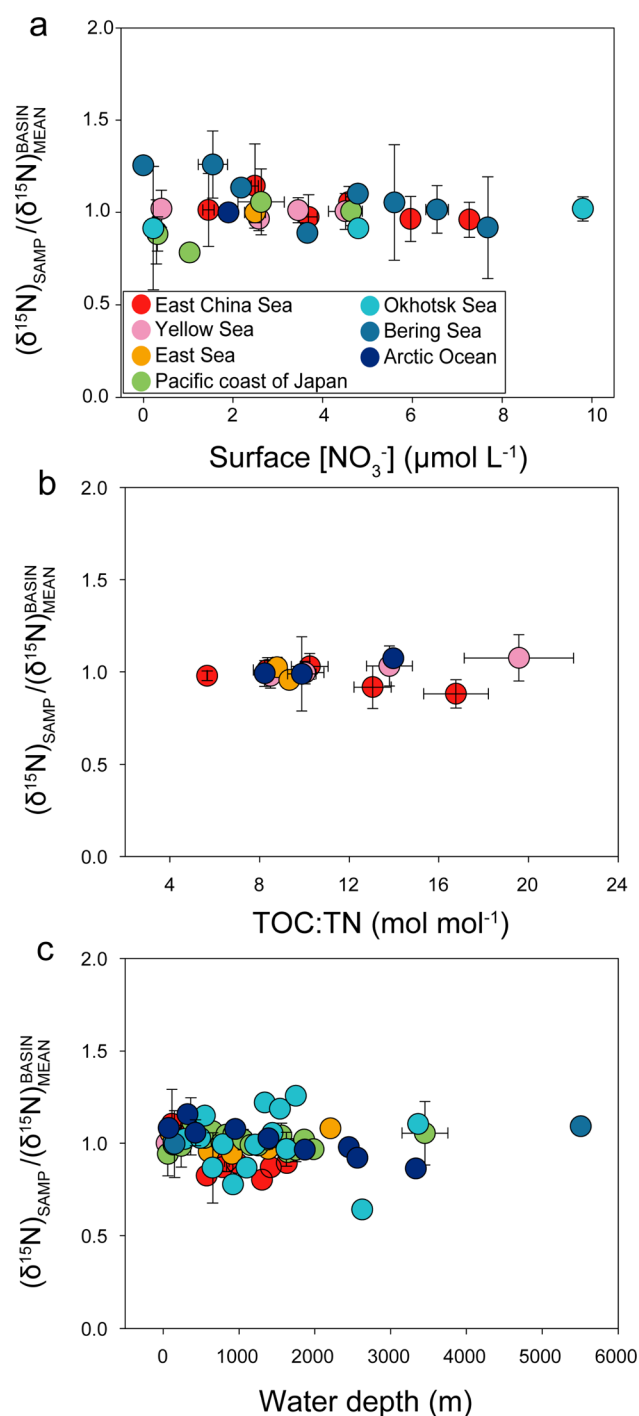


**Figure 4.** Sediment  $\delta^{15}\text{N}$  values as a function of  $[\text{NO}_3^-]$  ( $\mu\text{mol L}^{-1}$ ), TOC:TN ( $\text{mol mol}^{-1}$ ), and water depth ( $\text{m}$ ). The ratio of each sediment  $\delta^{15}\text{N}$  value ( $\delta^{15}\text{N}_{\text{SAMP}}$ ; ‰) to the corresponding basin-mean ( $\delta^{15}\text{N}_{\text{MEAN}}$ ; ‰) as a function of (a) spring mean concentration of surface nitrate ( $\mu\text{mol L}^{-1}$ ); (b) sediment TOC:TN ratio ( $\text{mol mol}^{-1}$ ); (c) water depth at which surface sediments were sampled ( $\text{m}$ ). No relationship between  $\delta^{15}\text{N}$  value and nitrate utilization (nitrate concentration), post digestion (TOC:TN ratio), and possible alteration by sinking (water depth).

northeast direction in our study area. However, even in the Yellow and East China seas, the regions of our study areas likely to exhibit the greatest effect of  $\text{N}_2$  fixation, Bashkin et al.<sup>15</sup> estimated  $\text{N}_2$  fixation to contribute only <7% of the contribution from atmospheric N deposition and riverine N

input; thus, the magnitude of  $\text{N}_2$  fixation across the study area is small. The advection of water (from the tropical western Pacific including the South China Sea) high in  $\text{N}_2$  fixation activity into the East China and Yellow seas may also lower water-column  $\delta^{15}\text{N}$  values and thereby lowering freshly produced POM  $\delta^{15}\text{N}$  values. However, the South China Sea already contained the  $\text{N}^{\text{ANTH}}$  component ( $61\text{--}87 \text{ mmol N m}^{-2} \text{ yr}^{-1}$ ),<sup>36–38</sup> which is far greater than the  $\text{N}_2$  fixation component ( $2.4\text{--}21 \text{ mmol N m}^{-2} \text{ yr}^{-1}$ ).<sup>39–41</sup>

Removal of the lighter  $^{14}\text{N}$  isotope through water column denitrification is another process that may have contributed to the northeastward increase in  $\delta^{15}\text{N}$ . This process would lower the abundance of  $^{14}\text{N}$  relative to  $^{15}\text{N}$  and thereby increase the surface water  $\delta^{15}\text{N}$ . Therefore, phytoplankton in high  $\delta^{15}\text{N}$  water would produce organic matter having high  $\delta^{15}\text{N}$  values and eventually increase the sediment  $\delta^{15}\text{N}$  value. If the level of water column denitrification increased in a northeast direction in the study area and was sufficiently large to change the surface  $\delta^{15}\text{N}$  to levels comparable to those observed in the sediments in our study, the effect of  $\text{N}^{\text{ANTH}}$  input may be dismissed. However, the denitrification rates of water column in the East China Sea ( $1.4\text{--}3.4 \text{ mmol N m}^{-2} \text{ d}^{-1}$ ) were found to be higher than those of the Okhotsk ( $0.8\text{--}1.1 \text{ mmol N m}^{-2} \text{ d}^{-1}$ ), Bering and Chukchi seas ( $0.8\text{--}1.7 \text{ mmol N m}^{-2} \text{ d}^{-1}$ ).<sup>42</sup> Therefore, we ruled out this process as an explanation for the northeastward increase in sediment  $\delta^{15}\text{N}$  values. In addition, if high-level  $\delta^{15}\text{N}$  water (caused by intensive denitrification) originating from the northeastern Pacific water were intruded into the Bering Sea, the sediment  $\delta^{15}\text{N}$  in the limited area of the Bering Sea bordering the Fe-limited Gulf of Alaska would have been higher than the levels found in the Arctic Ocean. However, the trend was found to be opposite to this. Therefore, the influence of intrusion of high levels of  $\delta^{15}\text{N}$ -nitrate into the Bering Sea, or further north into the Arctic Ocean, was probably insignificant. In some cases, high  $\delta^{15}\text{N}$  values have occasionally been reported for coastal sediments of the Bering Sea. These could in part be a result of the coupled sediment nitrification and denitrification processes, which preferentially remove  $^{14}\text{N}$ .<sup>43</sup> However, the occurrence of high values is an isolated phenomenon that does not significantly affect our interpretation.

The riverine input of terrestrial organic matter to the study area would bias sediment  $\delta^{15}\text{N}$  values if the contributions were substantial, because terrestrial organic matter has low  $\delta^{15}\text{N}$  values ( $0\text{--}5\text{‰}$ ).<sup>44</sup> Such an influence may be high in areas in close proximity of major rivers (i.e., Changjiang, Huang He, and Han rivers flowing into the East China and Yellow seas and Mackenzie and Yukon rivers flowing into the Chukchi Sea of the Arctic Ocean). Contrary to this hypothesis, all sediments sampled greater than 50 km distance from the mouth of the major rivers showed a  $\delta^{13}\text{C}$  value of  $-20\text{‰}$  and a TOC:TN ratio of  $<10.5$  ( $\text{mol mol}^{-1}$ ) (Table 3), providing robust evidence that the organic matter in the sediments was of marine origin.<sup>45–47</sup> The limited number of samples with a high TOC:TN ratio ( $>15 \text{ mol mol}^{-1}$ ; Figure 4b) observed in the East China and Yellow seas are indicative of a contribution of organic matter of terrestrial origin;<sup>45</sup> however, these data account for only <6% the total data points. In addition, studies based on a biomarker index (this method minimizes the biases associated with allochthonous inorganic N content and a wide range of  $\delta^{13}\text{C}$  values) showed that sedimentary organic matter from the East China, Yellow, and Chukchi seas was largely of marine origin.<sup>48–51</sup> Our measurements indicate that terrestrial

**Table 3.**  $\Delta^{13}\text{C}$  (‰) and TOC:TN ( $\text{mol mol}^{-1}$ ) Values for Surface Sediments Sampled >50 km Distance from the Mouth of the Major Rivers

basin	river	$\delta^{13}\text{C}_{\text{Pee Dee Belemnite}}$ (‰) ( $\pm\text{SD}$ )	TOC:TN ( $\text{mol mol}^{-1}$ ) ( $\pm\text{SD}$ )	no. of samples
East China Sea	Changjiang	$-20 \pm 0.8$	$9.0 \pm 1.8$	7
Yellow Sea	Huang He	$-21 \pm 1.0$	$9.7 \pm 1.6$	5
East Sea		$-21 \pm 0.4$	$9.1 \pm 0.5$	4
Arctic Ocean	Mackenzie and Yukon	$-24^a \pm 1.1$	$9.0 \pm 1.1$	4

<sup>a</sup>The  $\delta^{13}\text{C}$  of marine plankton in cold water was reported to be in the range of  $-25$  to  $-30$ ‰.<sup>45</sup>

organic matter was largely trapped in river and estuary before reaching the marine environment, and thus, the direct influence of terrestrial organic matter on our sediment  $\delta^{15}\text{N}$  values was probably minor.

Two other factors (i.e., the effects of a northeastward increase in the  $\delta^{15}\text{N}$ -nitrate value of the upwelled water and riverine discharge of Illite-bound ammonium into the study area) that may cause the observed northeastward increase in sediment  $\delta^{15}\text{N}$  were thoroughly examined in the [Supporting Information](#). Our analysis ruled out these factors as likely explanations.

In this analysis, we were unable to precisely estimate the contributions of all of the processes involved in determining sediment  $\delta^{15}\text{N}$  values. Such estimations will only be possible when  $\delta^{15}\text{N}$  measurements are performed on samples ranging from anthropogenic nitrate, water column, sinking fresh POM, and finally surface marine sediments. Such measurements are urgently needed to more accurately estimate and thus to confirm the role of  $\text{N}^{\text{ANTH}}$  in ocean regions under the influence of  $\text{N}^{\text{ANTH}}$ .

The lowered  $\delta^{15}\text{N}$  in the ocean regions with high  $\text{N}^{\text{ANTH}}$  input may indicate a shift in the major driver of biological export production. In the East China and Yellow seas and the East Sea, most added  $\text{N}^{\text{ANTH}}$  was assimilated and exported as organic matter and deposited in the sediments. The deposited organic matter eventually lowered the sediment  $\delta^{15}\text{N}$ . As a result, the greater decline in sediment  $\delta^{15}\text{N}$  compared to the baseline value indicates a greater contribution of  $\text{N}^{\text{ANTH}}$  to export production. Indeed, the large declines in sediment  $\delta^{15}\text{N}$  disclosed in the present study indicate that, in this region of the northwestern Pacific Ocean under the greatest influence of  $\text{N}^{\text{ANTH}}$ , biological export production is increasingly fueled by  $\text{N}^{\text{ANTH}}$  rather than nitrate flux from nitrate-rich deep water.

This study revealed a coherent sign of  $\text{N}^{\text{ANTH}}$  input, via planktonic assimilation and deposition, to the sedimentary environment of the nitrate-limited marginal seas of the northwestern Pacific Ocean, located downwind of the populated northeast Asian countries. This may have broader implications for future biological production and subsequent production of nitrous oxide in the marginal seas adjacent to China. Given that the magnitude of  $\text{N}^{\text{ANTH}}$  input will continue to increase in the future, this anthropogenic perturbation will increase primary production and the frequency and intensity of algal blooms. Increased algal blooms would increase export production of organic matter and subsequent remineralization, which in turn will increase nitrous oxide production by

potentially enhancing nitrification and denitrification, both in the water column and the sediments.

## ■ ASSOCIATED CONTENT

### Supporting Information

The Supporting Information is available free of charge on the [ACS Publications website](#) at DOI: [10.1021/acs.est.6b05316](https://doi.org/10.1021/acs.est.6b05316).

Details for methods, materials, and discussions ([PDF](#))

## ■ AUTHOR INFORMATION

### Corresponding Author

\*Phone: +82 54 279 2285. Fax: +82 54 279 8299. E-mail: [ktl@postech.ac.kr](mailto:ktl@postech.ac.kr).

### ORCID

Kitack Lee: [0000-0002-4226-2303](https://orcid.org/0000-0002-4226-2303)

### Notes

The authors declare no competing financial interest.

## ■ ACKNOWLEDGMENTS

The authors sincerely thank the scientists who contributed to the Nitrogen Cycle in the Ocean, Past and Present database (see Table S1; <http://www.ncdc.noaa.gov/paleo/pubs/nicopp/nicopp.html>),<sup>20</sup> atmospheric nitrogen deposition data (Oak Ridge National Laboratory Distributed Active Archive Center; <https://daac.ornl.gov/>),<sup>16</sup> and the surface ocean nitrate concentration data (the World Ocean Atlas 2013; <http://www.nodc.noaa.gov/OC5/woa13/woa13data.html>).<sup>24</sup> Sediment samples from the East China and Yellow seas were obtained from the Library of Marine Samples of South Sea Research Institute, Korea Institute of Ocean Science and Technology. This research was supported by Global Research Project (2013K1A1A2A02078278) and Midcareer Researcher Program (2015R1A2A1A05001847) funded by the NRF of Ministry of Science, ICT and Future Planning. Partial support was provided by “Management of Marine Organisms causing Ecological Disturbance and Harmful Effects” funded by the Ministry of Oceans and Fisheries. Seung-Il Nam was supported by the NRF of Ministry of Science, ICT, and Future Planning (2015M1A5A1037243).

## ■ REFERENCES

- (1) Duce, R. A.; LaRoche, J.; Altieri, K.; Arrigo, K. R.; Baker, A. R.; Capone, D. G.; Geider, R. J. Impacts of atmospheric anthropogenic nitrogen on the open ocean. *Science* **2008**, *320*, 893–897.
- (2) Kim, T. W.; Lee, K.; Najjar, R. G.; Jeong, H. D.; Jeong, H. J. Increasing N abundance in the Northwestern Pacific Ocean due to atmospheric nitrogen deposition. *Science* **2011**, *334*, 505–509.
- (3) Kim, I. N.; Lee, K.; Gruber, N.; Karl, D. M.; Bullister, J. L.; Yang, S.; Kim, T. W. Increasing anthropogenic nitrogen in the North Pacific Ocean. *Science* **2014**, *346*, 1102–1106.
- (4) Walters, W. W.; Goodwin, S. R.; Michalski, G. Nitrogen stable isotope composition ( $\delta^{15}\text{N}$ ) of vehicle-emitted  $\text{NO}_x$ . *Environ. Sci. Technol.* **2015**, *49*, 2278–2285.
- (5) Bateman, A. S.; Kelly, S. D. Fertilizer nitrogen isotope signature. *Isot. Environ. Health Stud.* **2007**, *43*, 237–247.
- (6) Sigman, D. M.; Altabet, M. A.; McCorkle, D. C.; François, R.; Fischer, G. The  $\delta^{15}\text{N}$  of nitrate in the Southern Ocean: Nitrogen cycling and circulation in the ocean interior. *J. Geophys. Res.* **2000**, *105*, 19599–19614.
- (7) Holtgrieve, G. W.; Schindler, D. E.; Hobbs, W. O.; Leavitt, P. R.; Ward, E. J.; Bunting, L.; Chen, G.; Finney, B. P.; Gregory-Eaves, I.; Holmgren, S.; Lisac, M. J. A coherent signature of anthropogenic



nitrogen deposition to remote watersheds of the northern hemisphere. *Science* **2011**, *334*, 1545–1548.

(8) Ruiz-Fernández, A. C.; Hillaire-Marcel, C.; Ghaleb, B.; Soto-Jiménez, M.; Páez-Osuna, F. Recent sedimentary history of anthropogenic impacts on the Culiacan River Estuary, northwestern Mexico: geochemical evidence from organic matter and nutrients. *Environ. Pollut.* **2002**, *118*, 365–377.

(9) Barros, G. V.; Martinelli, L. A.; Novais, T. O.; Ometto, J. H. B.; Zuppi, G. M. Stable isotopes of bulk organic matter to trace carbon and nitrogen dynamics in an estuarine ecosystem in Babitonga Bay (Santa Catarina, Brazil). *Sci. Total Environ.* **2010**, *408*, 2226–2232.

(10) Gao, X.; Yang, Y.; Wang, C. Geochemistry of organic carbon and nitrogen in surface sediments of coastal Bohai Bay inferred from their ratios and stable isotopic signatures. *Mar. Pollut. Bull.* **2012**, *64*, 1148–1155.

(11) Altabet, M. A.; Francois, R.; Murray, D. W.; Prell, W. L. Climate related variations in denitrification in the Arabian Sea from sediment  $^{15}\text{N}/^{14}\text{N}$  ratios. *Nature* **1995**, *373*, 506–509.

(12) Farrell, J. W.; Pedersen, T. F.; Calvert, S. E.; Nielsen, B. Glacial-interglacial changes in nutrient utilization in the equatorial Pacific Ocean. *Nature* **1995**, *377*, 514–517.

(13) Altabet, M. A.; Francois, R. Nitrogen isotope biogeochemistry of the Antarctic polar frontal zone at  $170^\circ\text{W}$ . *Deep Sea Res., Part II* **2001**, *48*, 4247–4273.

(14) Dai, Z.; Du, J.; Zhang, X.; Su, N.; Li, J. Variation of riverine material loads and environmental consequences on the Changjiang (Yangtze) estuary in recent decades (1950–2008). *Environ. Sci. Technol.* **2011**, *45*, 223–227.

(15) Bashkin, V. N.; Park, S. U.; Choi, M. S.; Lee, C. B. Nitrogen budgets for the Republic of Korea and the Yellow Sea region. *Biogeochemistry* **2002**, *57*, 387–403.

(16) Dentener, F. J. *Global Maps of Atmospheric Nitrogen Deposition, 1860, 1993, and 2050*; Data set; Oak Ridge National Laboratory Distributed Active Archive Center: Oak Ridge, TN, 2006; DOI:10.3334/ORNLDAAAC/830.

(17) Hails, J. R. Grab samplers. *Beach. Coastal Geol.* **1982**, *7*, 454–455.

(18) Huh, C. A.; Su, C. C. Sedimentation dynamics in the East China Sea elucidated from  $^{210}\text{Pb}$ ,  $^{137}\text{Cs}$ ,  $^{239,240}\text{Pu}$ . *Mar. Geol.* **1999**, *160*, 183–196.

(19) Lim, D. I.; Choi, J. Y.; Jung, H. S.; Rho, K. C.; Ahn, K. S. Recent sediment accumulation and origin of shelf mud deposits in the Yellow and East China Seas. *Prog. Oceanogr.* **2007**, *73*, 145–159.

(20) Tesdal, J. E.; Galbraith, E. D.; Kienast, M. Nitrogen isotopes in bulk marine sediment: linking seafloor observations with subseafloor records. *Biogeosciences* **2013**, *10*, 101–118.

(21) Sharp, Z. *Principles of stable isotope geochemistry*; Prentice Hall: New Jersey, USA, 2005.

(22) Stable Isotope Facility at University of California Web site. <http://stableisotopefacility.ucdavis.edu/13cand15n.html> (accessed May 4, 2017).

(23) Nelson, D. W.; Sommers, L. E. Part 3. Chemical methods. In *Methods of soil analysis*; Sparks, D. R., Eds.; Soil Science Society of America: Madison, WI, 1996.

(24) Boyer, T. P.; Antonov, J. I.; Baranova, O. K.; Garcia, H. E.; Johnson, D. R.; Mishonov, A. V.; O'Brien, T. D.; et al. World Ocean Database 2013. In *NOAA Atlas NESDIS 72*; Levitus, S., Ed.; Mishonov, A., Technical Ed.; Silver Spring: WA, 2013; DOI:10.7289/VSNZ85MT.

(25) Hannides, C. C. S.; Popp, B. N.; Choy, C. A.; Drazen, J. C. Midwater zooplankton and suspended particle dynamics in the North Pacific Subtropical Gyre: A stable isotope perspective. *Limnol. Oceanogr.* **2013**, *58*, 1931–1946.

(26) Smith, S. L.; Henrichs, S. M.; Rho, T. Stable C and N isotopic composition of sinking particles and zooplankton over the south-eastern Bering Sea shelf. *Deep Sea Res., Part II* **2002**, *49*, 6031–6050.

(27) Holmes, M. E.; Lavik, G.; Fischer, G.; Wefer, G. Nitrogen Isotopes in Sinking Particles and Surface Sediments in the Central and Southern Atlantic. In *The South Atlantic in the Late Quaternary*;

*Reconstruction of Material Budgets and Current Systems*; Wefer, G., Mulitza, S., Ratmeyer, V., Eds.; Springer Berlin Heidelberg: Berlin, 2004; pp 143–165, DOI: 10.1007/978-3-642-18917-3\_8.

(28) Jia, G.; Chen, F. Monthly variations in nitrogen isotopes of ammonium and nitrate in wet deposition at Guangzhou, south China. *Atmos. Environ.* **2010**, *44*, 2309–2315.

(29) Seitzinger, S. J.; Harrison, J. A. Land-based nitrogen sources and their delivery to coastal systems. In *Nitrogen in the marine environment*; Douglas, G. C., Deborah, A. B., Margaret, R. M., Edward, J. C., Eds.; Academic Press: Cambridge, 2008; pp 469–540.

(30) Kendall, C.; Elliott, E. M.; Wankel, S. D. Tracing anthropogenic inputs of nitrogen ecosystem. In *Stable Isotopes in Ecology and Environmental Science*; Michener, R., Lajtha, K., Eds.; Wiley-Blackwell: Hoboken, New Jersey, 2007; pp 375–449, DOI: 10.1002/9780470691854.ch12.

(31) Akimoto, H.; Narita, H. Distribution of  $\text{SO}_2$ ,  $\text{NO}_x$  and  $\text{CO}_2$  emissions from fuel combustion and industrial activities in Asia with  $1\times 1$  resolution. *Atmos. Environ.* **1994**, *28*, 213–225.

(32) Ohara, T. A. H. K.; Akimoto, H.; Kurokawa, J. I.; Horii, N.; Yamaji, K.; Yan, X.; Hayasaka, T. An Asian emission inventory of anthropogenic emission sources for the period 1980–2020. *Atmos. Chem. Phys.* **2007**, *7*, 4419–4444.

(33) Ryabenko, E. Stable isotope methods for the study of the nitrogen cycle. In *Topics in Oceanography*; Zambianchi, E., Eds.; InTech: Croatia, 2013; pp 1–40, DOI: 10.5772/56105.

(34) Robinson, R. S.; Kienast, M.; Luiza Albuquerque, A.; Altabet, M.; Contreras, S.; De Pol Holz, R.; Dubois, N.; Francois, R.; Galbraith, E.; Hsu, T. C.; Ivanochko, T. A review of nitrogen isotopic alteration in marine sediments. *Paleoceanography* **2012**, *27*, PA4203.

(35) Brahney, J.; Ballantyne, A. P.; Turner, B. L.; Spaulding, S. A.; Otu, M.; Neff, J. C. Separating the influences of diagenesis, productivity and anthropogenic nitrogen deposition on sedimentary  $\delta^{15}\text{N}$  variations. *Org. Geochem.* **2014**, *75*, 140–150.

(36) Liu, S. M.; Hong, G. H.; Zhang, J.; Ye, X. W.; Jiang, X. L. Nutrient budgets for large Chinese estuaries. *Biogeosciences* **2009**, *6*, 2245–2263.

(37) Grosse, J.; Bombar, D.; Doan, H. N.; Nguyen, L. N.; Voss, M. The Mekong River plume fuels nitrogen fixation and determines phytoplankton species distribution in the South China Sea during low- and high-discharge season. *Limnol. Oceanogr.* **2010**, *55*, 1668–1680.

(38) Kim, T. W.; Lee, K.; Duce, R.; Liss, P. Impact of atmospheric nitrogen deposition on phytoplankton productivity in the South China Sea. *Geophys. Res. Lett.* **2014**, *41*, 3156–3162.

(39) Chen, Y. I. L.; Chen, H. Y.; Karl, D. M.; Takahashi, M. Nitrogen modulates phytoplankton growth in spring in the South China Sea. *Cont. Shelf Res.* **2004**, *24*, 527–541.

(40) Chen, Y. I. L.; Chen, H. Y.; Tuo, S. H.; Ohki, K. Seasonal dynamics of new production from *Trichodesmium*  $\text{N}_2$  fixation and nitrate uptake in the upstream Kuroshio and South China Sea basin. *Limnol. Oceanogr.* **2008**, *53*, 1705–1721.

(41) Voss, M.; Bombar, D.; Loick, N.; Dippner, J. W. Riverine influence on nitrogen fixation in the upwelling region off Vietnam, South China Sea. *Geophys. Res. Lett.* **2006**, *33*, L07604.

(42) Seitzinger, S.; Harrison, J. A.; Böhlke, J. K.; Bouwman, A. F.; Lowrance, R.; Peterson, B.; Tobias, C.; Drecht, G. V. Denitrification across landscapes and watersheds: A synthesis. *Ecol. Appl.* **2006**, *16*, 2064–2090.

(43) Granger, J.; Prokopenko, M. G.; Sigman, D. M.; Mordy, C. W.; Morse, Z. M.; Morales, L. V.; Sambrotto, R. N.; Plessen, B. Coupled nitrification-denitrification in sediment of the eastern Bering Sea shelf leads to  $^{15}\text{N}$  enrichment of fixed N in shelf waters. *J. Geophys. Res.* **2011**, *116*, C11006.

(44) Montoya, J. P. Nitrogen stable isotopes in marine environments. In *Nitrogen in the marine environment*; Douglas, G. C., Deborah, A. B., Margaret, R. M., Edward, J. C., Eds.; Academic Press: Cambridge, 2008; pp 1277–1302, DOI: 10.1016/B978-0-12-372522-6.00029-3.

(45) Sackett, W. Stable carbon isotope studies on organic matter in the marine environment. In *Handbook of environmental isotope geochemistry*; Baskaran, M., Eds.; Elsevier Science: Amsterdam, 1989.



- (46) Rumolo, P.; Barra, M.; Gherardi, S.; Marsella, E.; Sprovieri, M. Stable isotopes and C/N ratios in marine sediments as a tool for discriminating anthropogenic impact. *J. Environ. Monit.* **2011**, *13*, 3399–3408.
- (47) Khan, N. S.; Vane, C. H.; Horton, B. P. Stable carbon isotope and C/N geochemistry of coastal wetland sediments as a sea-level indicator. In *Handbook of sea-level research*; Shennan, I., Long, A. J., Horton, B. P., Eds.; John Wiley and Sons: Chichester, 2015; DOI: [10.1002/9781118452547.ch20](https://doi.org/10.1002/9781118452547.ch20).
- (48) Xing, L.; Zhang, H.; Yuan, Z.; Sun, Y.; Zhao, M. Terrestrial and marine biomarker estimates of organic matter sources and distributions in surface sediments from the East China Sea shelf. *Cont. Shelf Res.* **2011**, *31*, 1106–1115.
- (49) Xing, L.; Tao, S.; Zhang, H.; Liu, Y.; Yu, Z.; Zhao, M. Distributions and origins of lipid biomarkers in surface sediments from the southern Yellow Sea. *Appl. Geochem.* **2011**, *26*, 1584–1593.
- (50) Belicka, L. L.; Macdonald, R. W.; Harvey, H. R. Sources and transport of organic carbon to shelf, slope, and basin surface sediments of the Arctic Ocean. *Deep Sea Res., Part I* **2002**, *49*, 1463–1483.
- (51) Belicka, L. L.; Macdonald, R. W.; Yunker, M. B.; Harvey, H. R. The role of depositional regime on carbon transport and preservation in Arctic Ocean sediments. *Mar. Chem.* **2004**, *86*, 65–88.
- (52) Hong, G. H.; Kim, S. H.; Chung, C. S.; Kang, D. J.; Shin, D. H.; Lee, H. J.; Han, S. J. <sup>210</sup>Pb-derived sediment accumulation rates in the southwestern East Sea (Sea of Japan). *Geo-Mar. Lett.* **1997**, *17*, 126–132.
- (53) Lee, T. H.; Hyun, J. H.; Mok, J. S.; Kim, D. S. Organic carbon accumulation and sulfate reduction rates in slope and basin sediments of the Ulleung Basin, East/Japan Sea. *Geo-Mar. Lett.* **2008**, *28*, 153–159.
- (54) Okazaki, Y.; Takahashi, K.; Katsuki, K.; Ono, A.; Hori, J.; Sakamoto, T.; Uchida, M.; Shibata, Y.; Ikehara, M.; Aoki, K. Late quaternary paleoceanographic changes in the southwestern Okhotsk Sea: Evidence from geochemical, radiolarian, and diatom records. *Deep Sea Res., Part II* **2005**, *52*, 2332–2350.
- (55) Sugisaki, S.; Buylaert, J. P.; Murray, A. S.; Harada, N.; Kimoto, K.; Okazaki, Y.; Sakamoto, T.; Iijima, K.; Tsukamoto, S.; Miura, H.; Nogi, Y. High resolution optically stimulated luminescence dating of a sediment core from the southwestern Sea of Okhotsk. *Geochem., Geophys., Geosyst.* **2012**, *13*, Q0AA22.
- (56) Seki, O.; Ikehara, M.; Kawamura, K.; Nakatsuka, T.; Ohnishi, K.; Wakatsuchi, M.; Narita, H.; Sakamoto, T. Reconstruction of paleoproductivity in the Sea of Okhotsk over the last 30 kyr. *Paleoenography* **2004**, *19*, PA1016.
- (57) Tsunogai, S.; Yamada, M. <sup>326</sup>Ra in Bering Sea sediment and its application as a geochronometer. *Geochem. J.* **1979**, *13*, 231–238.
- (58) Huh, C. A.; Pisias, N. G.; Kelley, J. M.; Maiti, T. C.; Grantz, A. Natural radionuclides and plutonium in sediments from the western Arctic Ocean: sedimentation rates and pathways of radionuclides. *Deep Sea Res., Part II* **1997**, *44*, 1725–1743.
- (59) Bian, C.; Wensheng, J.; Greatbatch, R. J.; Hui, H. The suspended sediment concentration distribution in the Bohai Sea, Yellow Sea and East China Sea. *J. Ocean Univ. China* **2013**, *12*, 345–354.
- (60) Fry, B. Isotope Chi. In *Stable isotope ecology*; Fry, B., Eds.; Springer: New York, 2008; pp 76–118.
- (61) Yu, H.; Yu, Z.; Song, X.; Cao, X.; Yuan, Y.; Lu, G. Seasonal variations in the nitrogen isotopic composition of dissolved nitrate in the Changjiang River estuary, China. *Estuarine, Coastal Shelf Sci.* **2015**, *155*, 148–155.
- (62) Kao, S. J.; Lin, F. J.; Liu, K. K. Organic carbon and nitrogen contents and their isotopic compositions in surficial sediments from the East China Sea shelf and the southern Okinawa Trough. *Deep Sea Res., Part II* **2003**, *50*, 1203–1217.
- (63) Wang, Y.; Liu, D.; Richard, P.; Li, X. A geochemical record of environmental changes in sediments from Sishili Bay, northern Yellow Sea, China: Anthropogenic influence on organic matter sources and composition over the last 100 years. *Mar. Pollut. Bull.* **2013**, *77*, 227–236.